



**HAL**  
open science

# Coordination-Driven Construction of Porphyrin Nanoribbons at a Highly Oriented Pyrolytic Graphite (HOPG)/Liquid Interface

Mary-Ambre Carvalho, Hervé Dekkiche, Mayumi Nagasaki, Yoshihiro Kikkawa, Romain Ruppert

► **To cite this version:**

Mary-Ambre Carvalho, Hervé Dekkiche, Mayumi Nagasaki, Yoshihiro Kikkawa, Romain Ruppert. Coordination-Driven Construction of Porphyrin Nanoribbons at a Highly Oriented Pyrolytic Graphite (HOPG)/Liquid Interface. *Journal of the American Chemical Society*, 2019, 141 (26), pp.10137-10141. 10.1021/jacs.9b02145 . hal-02175658

**HAL Id: hal-02175658**

**<https://hal.science/hal-02175658v1>**

Submitted on 5 Jul 2019

**HAL** is a multi-disciplinary open access archive for the deposit and dissemination of scientific research documents, whether they are published or not. The documents may come from teaching and research institutions in France or abroad, or from public or private research centers.

L'archive ouverte pluridisciplinaire **HAL**, est destinée au dépôt et à la diffusion de documents scientifiques de niveau recherche, publiés ou non, émanant des établissements d'enseignement et de recherche français ou étrangers, des laboratoires publics ou privés.

## 1 Coordination-Driven Construction of Porphyrin Nanoribbons at a 2 Highly Oriented Pyrolytic Graphite (HOPG)/Liquid Interface

3 Mary-Ambre Carvalho,<sup>†</sup> Hervé Dekkiche,<sup>†</sup> Mayumi Nagasaki,<sup>‡</sup> Yoshihiro Kikkawa,<sup>\*,‡,§</sup>  
4 and Romain Ruppert<sup>\*,†,§</sup>

5 <sup>†</sup>Institut de Chimie, UMR 7177 du CNRS, Université de Strasbourg, 4 rue Blaise Pascal, 67000 Strasbourg, France

6 <sup>‡</sup>National Institute of Advanced Industrial Science and Technology (AIST), 1-1-1 Higashi, Tsukuba, Ibaraki 305-8565, Japan

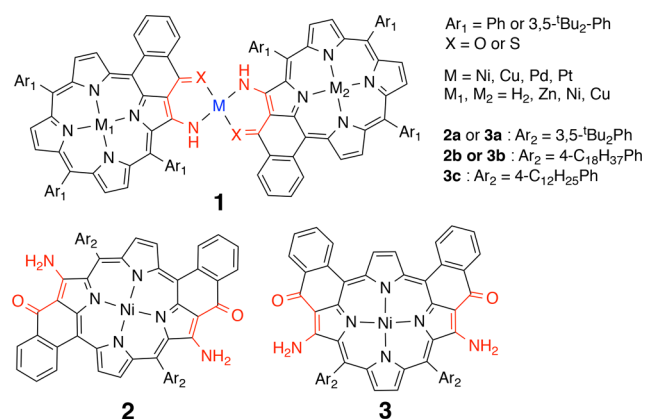
7 **S** Supporting Information

8 **ABSTRACT:** Nanostructures were built at the solid/  
9 liquid interface by self-assembly and/or coordination  
10 bonds. Metalloporphyrins bearing two external coordina-  
11 tion sites and long alkyl chains allowed the self-assembly  
12 of the compounds on highly oriented pyrolytic graphite.  
13 After addition of a metal ion, long transition-metal linked  
14 porphyrin nanoribbons were obtained and visualized by  
15 scanning tunneling microscopy. In these porphyrin  
16 ribbons electronic delocalization is possible through the  
17 d orbitals of the connecting metal ions.

18 **B**uilding well-ordered supramolecular architectures from  
19 functional subunits might be potentially useful for  
20 applications in (opto)electronics, magnetism, energy harvest-  
21 ing, or smart coatings. The bottom-up synthesis is an  
22 interesting method to obtain such ordered nanomaterials by  
23 using noncovalent interactions. This strategy was discussed  
24 two decades ago by leading scientists.<sup>1,2</sup> In particular, using  
25 these approaches to prepare nanowires or nanotubes will be of  
26 importance for future technological applications. Porphyrins  
27 are good candidates for the construction of nanostructures in  
28 many fields of applications due to their interesting optoelec-  
29 tronic properties. The synthesis of long conjugated porphyrin  
30 wires using covalent linkages was started more than two  
31 decades ago. Triple bonds as connecting functions were the  
32 most widely used because strong electronic or magnetic  
33 interactions occur between the subunits.<sup>3,4</sup> At the beginning of  
34 this century, the Osuka group synthesized very long conjugated  
35 porphyrin tapes, in which the individual porphyrins are fused  
36 and linked by three covalent bonds.<sup>5</sup> However, the syntheses of  
37 all these molecules often remain a challenge and therefore  
38 preclude possible practical applications.

39 It was possible to assemble porphyrins bearing external  
40 coordination sites with metal ions in solution.<sup>6</sup> Strong  
41 electronic interactions were demonstrated between the  
42 individual subunits in porphyrin dimers (see **1** in **Chart 1**,  
43 top) by using enamino(thio)ketones as ligands for the  
44 connecting ions. These external coordination sites can also  
45 be described as noninnocent ligands, thus allowing electronic  
46 delocalization over the entire molecule through the d orbitals  
47 of the linking metal ion, and this was corroborated by DFT  
48 studies.<sup>7</sup> Larger molecules were obtained by using porphyrins  
49 bearing two external coordination sites (examples of such

**Chart 1. Porphyrin Dimers 1 Linked by Metal Ions (Top);  
Two Porphyrin Monomers Used in This Study: 2 with a  
Center of Symmetry and 3 with a Plane of Symmetry  
(Bottom)**



50 molecules used in these studies are shown in **Chart 1**, **2a** and  
51 **3a** (bottom).<sup>8,9</sup>

52 However, the selective preparation of molecules containing  
53 more than three or four porphyrins by this coordination  
54 chemistry linkage approach proved to be as challenging as the  
55 covalent bond formation approach.

56 On-surface synthesis to obtain new functional molecules has  
57 attracted intense attention over the past decade. Steering the  
58 reaction outcome and improving the chemo- and regioselec-  
59 tivity during these processes remain a real challenge because it  
60 is difficult to modify the reaction parameters under UHV  
61 conditions.<sup>10</sup> Most previous studies were conducted on  
62 metallic surfaces at relatively high temperatures to obtain  
63 potential functional nanostructures containing conjugated  
64 molecules, polyaromatics, or even oligoporphyrins.<sup>11–15</sup> The  
65 on-surface approach, but under much milder reaction  
66 conditions, in solvents and using noncovalent bond forming  
67 reactions as assembling tools at a liquid/HOPG interface was  
68 therefore considered by different groups.<sup>16–19</sup> The self-  
69 assembled structures have been revealed by using scanning  
70 tunneling microscopy<sup>20,21</sup> (STM) at the solid/liquid inter-  
71 face.<sup>22–24</sup> Well-organized structures can be generated this way,

**Received:** February 25, 2019

**Published:** June 11, 2019

72 but interactions between the individual units are generally  
73 rather small.<sup>25–34</sup>

74 Porphyrin monomers or presynthesized dimers such as **1**  
75 bearing long alkoxy chains self-assembled at the liquid/highly  
76 oriented pyrolytic graphite (HOPG) surface.<sup>9</sup> To prepare  
77 higher oligoporphyrins linked by metal ions, porphyrins  
78 bearing two external coordination sites in addition to long  
79 *meso*-alkylphenyl groups are needed. The *Ar meso* substituents  
80 used in the present studies were phenyl groups bearing C<sub>18</sub>H<sub>37</sub>  
81 alkyl chains in the *para* positions (Ph–C<sub>18</sub>H<sub>37</sub>). To obtain  
82 linear porphyrin ribbons, two series of symmetrical porphyrin  
83 **2** and **3** (with a center or a plane of symmetry) were used for  
84 the self-assembly process. Porphyrins such as **2b** and **3b** were  
85 obtained by following procedures used earlier for the  
86 preparation of similar porphyrins (see Supporting Information  
87 (SI) for experimental details).

88 Before starting the on-surface studies, we had noticed in the  
89 X-ray structure of compound **3c** that linear tapes with  
90 molecules held together by hydrogen bonds were present  
91 (see Figure 1). In the solid state, the molecules of **3c** (bearing

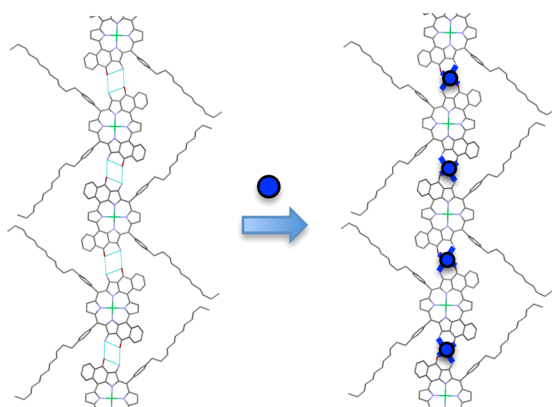


**Figure 1.** X-ray structure of compound **3c** (Ar = PhC<sub>12</sub>H<sub>25</sub>). Hydrogen bonds between the individual porphyrins are schematically drawn in light blue,  $d(\text{Ni}-\text{Ni}) = 14.339 \text{ \AA}$  (left). Right: expected formation of nickel(II)-connected porphyrin nanoribbons.

92 two Ph–C<sub>12</sub>H<sub>25</sub> *meso* groups) are arranged in such a way that  
93 the two external coordination sites were already preorganized  
94 to build square planar metal complexes if divalent metal ions  
95 are added.<sup>35</sup> Similar arrangements of porphyrin **3b** at the  
96 solid/liquid interface were therefore expected, and the  
97 construction of linear ribbons with porphyrins linked by  
98 metal ions could be envisaged directly at the interface  
99 (according to the schematic representation shown in Figure  
100 **1** at the right).

101 Drop casting a phenyloctane solution of porphyrin **3b** onto a  
102 HOPG surface gave a well-organized arrangement of the  
103 porphyrins at the solid/liquid interface. However, the additional  
104 interactions of the alkyl chains with the hexagonal  
105 HOPG surface led to a different arrangement of the molecules  
106 than in the solid-state structure. Two porphyrins were  
107 assembled in centro-symmetric pairs held together by  
108 hydrogen bonds, and all pairs were separated by a space (see  
109 Figure 2a and 2b).

110 Apart from this observation, the expected alternating  
111 arrangement of molecules was present at the interface and  
112 the porphyrins were aligned in rows separated by spaces filled  
113 by the alkyl chains that interact with HOPG. The distance ( $L_1$   
114 in Figure 2b) between the porphyrin rows was  $2.8 \pm 0.1 \text{ nm}$ .

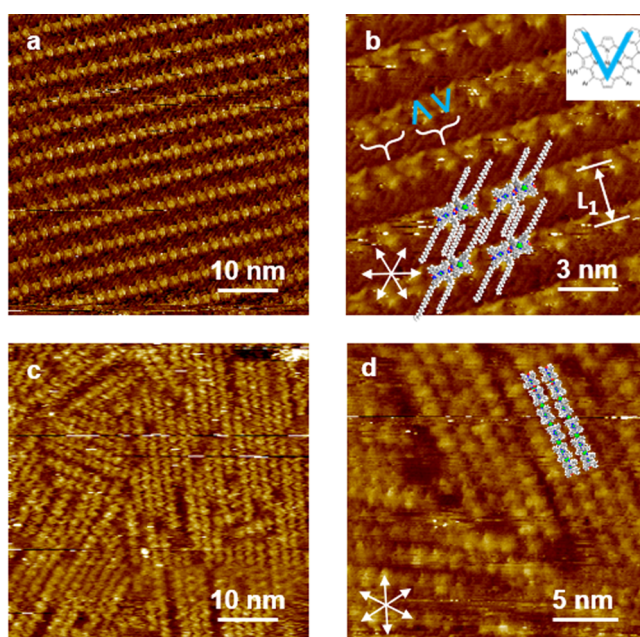


**Figure 2.** STM height images of compound **3b** (Ar = PhC<sub>18</sub>H<sub>37</sub>) before (a, b) and after the addition of nickel(II) (c, d) at the HOPG/phenyloctane interface ( $c = 1 \text{ mM}$ ). Pairs are highlighted with brackets in (b). Proposed molecular models were superimposed on the STM images in (b) and (d). In (d), the C<sub>18</sub> alkyl chains were replaced by CH<sub>3</sub> groups. Arrows indicate the HOPG lattice directions. Tunneling conditions: (a)  $I = 1.1 \text{ pA}$ ,  $V = -103 \text{ mV}$ , (b)  $I = 1.2 \text{ pA}$ ,  $V = -164 \text{ mV}$ , (c)  $I = 1.6 \text{ pA}$ ,  $V = -989 \text{ mV}$ , (d)  $I = 1.4 \text{ pA}$ ,  $V = -818 \text{ mV}$ .

The C<sub>18</sub> alkyl chains were sandwiched between the porphyrin  
115 rows with an angle of ca. 40°. Varying the concentration of the  
116 porphyrin **3b** down to 0.1 mM gave similar arrangements at  
117 the interface (see SI). It should be emphasized at this point  
118 that these very ruffled porphyrins<sup>36</sup> are functionalized with  
119 only two C<sub>18</sub>H<sub>37</sub> alkyl chains, thus necessitating the use of  
120 rather high concentrations (from 0.05 to 1 mM). Addition of  
121 an equimolar amount of nickel(II) (Ni(acac)<sub>2</sub> in CH<sub>2</sub>Cl<sub>2</sub>/  
122 phenyloctane) drastically changed the arrangement of the  
123 molecules at the interface. We noticed in the early stage of this  
124 study that these arrangements also evolved over time after the  
125 addition of the metal salt and that the equilibrium was reached  
126 after approximately 1 h. Figure 2c and 2d show the  
127 arrangements of porphyrin **3b** 1 h after addition of nickel(II).  
128 The formation of long linear ribbons (maximum length ca. 30  
129 nm) of porphyrins linked by nickel(II) can be visualized in  
130 Figure 2d. Note that similar observations of linear ribbons were  
131 available for both a premixed solution of Ni(II) and **3b** as well  
132 as after *in situ* addition of Ni(II) to the deposited solution of  
133 **3b** on the HOPG surface. These results suggest that oligomers  
134 observed for the *in situ* experiment might be preferentially  
135 formed in solution and then compete with monomers  
136 adsorbed at the interface.  
137

At the 1 mM concentration, most of the individual ribbons  
138 were not separated by alkyl chain areas and were densely  
139 packed at the interface (Figure 3a), as shown by the measured  
140 distance between the neighboring ribbons ( $L_2 = 1.6 \pm 0.1 \text{ nm}$ ;  
141 Figure 3b). The interactions of the long aromatic systems with  
142 HOPG were large enough to keep the linear arrays on HOPG,  
143 and the alkyl chains were oriented toward the solution.  
144 Lowering stepwise the concentration from 1 mM to 0.05 mM  
145



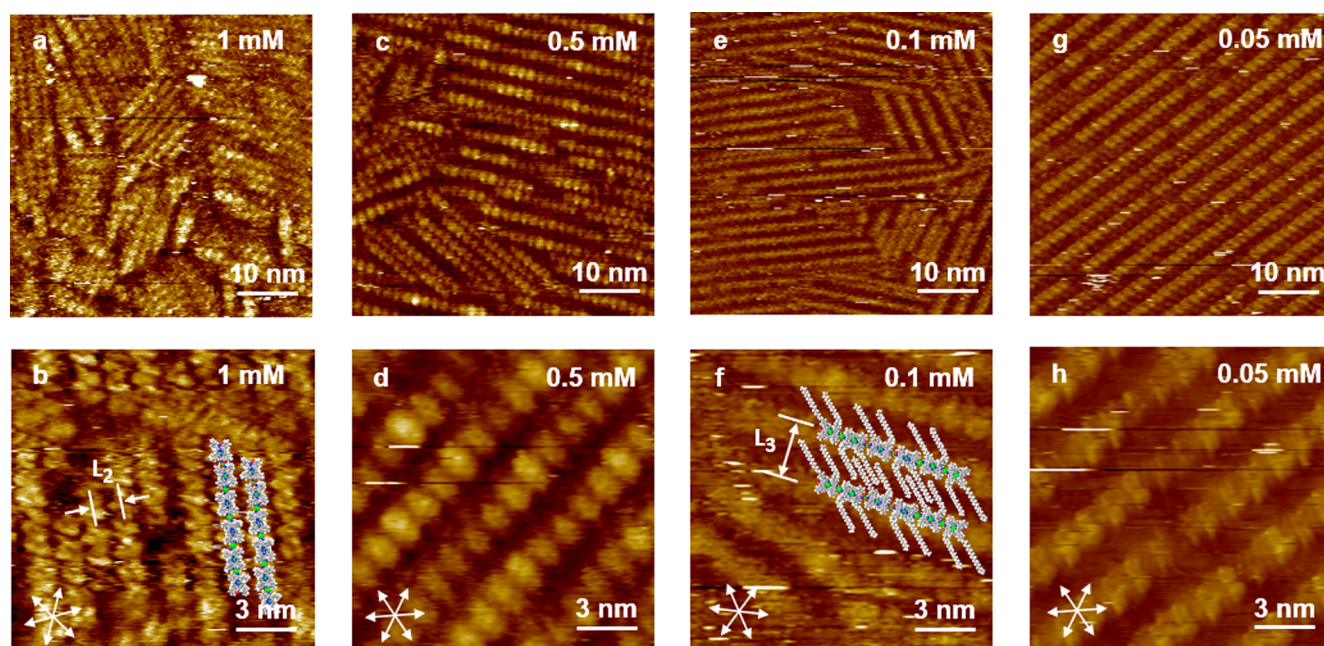


**Figure 3.** STM height images of porphyrin **3b** at different concentrations after addition of 1 equiv of nickel(II). Assuming a similar orientation of the alkyl chains (as in Figure 2b), a molecular model of linear ribbons with sparse packing was superimposed on the STM image in (f). Concentrations of the solution are indicated on each STM image. Tunneling conditions: (a)  $I = 1.0$  pA,  $V = -752$  mV, (b)  $I = 2.0$  pA,  $V = -948$  mV, (c)  $I = 1.9$  pA,  $V = -740$  mV, (d)  $I = 3.8$  pA,  $V = -823$  mV, (e)  $I = 2.4$  pA,  $V = -942$  mV, (f)  $I = 3.1$  pA,  $V = -744$  mV, (g)  $I = 1.0$  pA,  $V = -1000$  mV, (h)  $I = 5.0$  pA,  $V = -1000$  mV.

146 gave images with more sparsely packed areas (see Figure 3). At  
 147 a concentration of 0.1 mM, well-separated ribbons were  
 148 formed almost exclusively. The distance  $L_3$  between them was  
 149  $2.7 \pm 0.1$  nm, which was almost identical to the value of  $L_1$   
 150 found for **3b** without Ni(II). This result suggests that the  
 151 nanoribbons are adsorbed on the HOPG with the assistance of  
 152 alkyl chains, which are packed between the porphyrin rows.

153 It is not possible to compare studies in solution with studies  
 154 at the HOPG/liquid interface. However, in order to have an  
 155 idea of the electronic structure of the linear arrays at the  
 156 surface, solution experiments were performed at concen-  
 157 trations close to those used earlier to generate the nanoribbons  
 158 at the interface. An equimolar amount of Ni(acac)<sub>2</sub> was added  
 159 to a toluene solution of porphyrin **3b** in a thin quartz cell. The  
 160 electronic spectrum was recorded as a function of time. The  
 161 results of the first measurements are depicted in Figure 4. As  
 162 the complexation reaction progressed in solution, a batho-  
 163 chromic shift of all absorption bands was observed. The

164 reaction could not be monitored to completion because the  
 165 metal ion linked oligoporphyrins formed after addition of  
 166 Ni(acac)<sub>2</sub> were also adsorbed on the quartz faces of the  
 167 cuvette, giving rise to light-diffusion phenomena. However, the  
 168 evolution of the first four spectra clearly indicated that strong  
 169 interactions between porphyrin subunits linked by nickel(II)  
 170 ions were present in the oligoporphyrins. A flattening and  
 171 broadening of the bands in the Soret area (from 450 to 600  
 172 nm) and a bathochromic shift of the Q bands to wavelengths  
 173 higher than 900 nm are the signature of strong electronic  
 174 interactions between the aromatic  $\pi$ -electrons of each  
 175 individual porphyrin induced by the participation of the d  
 176 orbitals of the linking metal ions.

177 To demonstrate that this approach was not limited to  
 178 porphyrin **3b**, centro-symmetric porphyrin monomer **2b** (Ar =  
 179 PhC<sub>18</sub>H<sub>37</sub>) was also prepared. Once more, the self-assembly of  
 180 the individual molecules was studied at the HOPG/liquid  
 181 interface. The STM images obtained for millimolar phenyl-  
 182 octane solutions of **2b** were not as well resolved as for  
 183 porphyrin **3b** (see Figure 5a). However, to see if the  
 184 oligoporphyrins could be constructed and visualized at the  
 185 interface, the same procedure described earlier for **3b** was  
 186 followed. The STM images in Figure 5b clearly showed that,  
 187 again, long linear nanoribbons of porphyrins were present at  
 188 the interface. As observed before for **3b**, large areas of the  
 189 surface were occupied by alkyl chains for monomer **2b**, but  
 190 upon addition of Ni(acac)<sub>2</sub>, the porphyrin nanoribbons were  
 191 again densely packed on the surface.

192 In conclusion, we have demonstrated that long linear  
 193 porphyrin nanoribbons can be constructed at the HOPG/  
 194 liquid interface by using a combination of weak interactions  
 195 (hydrogen bonds, van der Waals interactions with the surface  
 196 and/or between alkyl chains) and also stronger coordination  
 197 linkages. By combining these two factors, the best of both

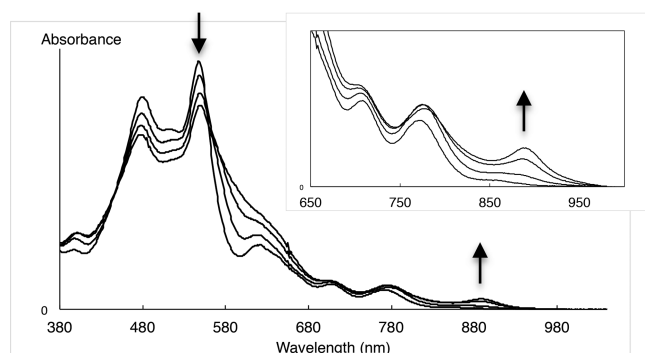


**Figure 4.** Electronic spectra of monomer **3b** as a function of time after addition of 1 equiv of Ni(acac)<sub>2</sub> in toluene ( $t = 0, 5, 20,$  and  $60$  min).

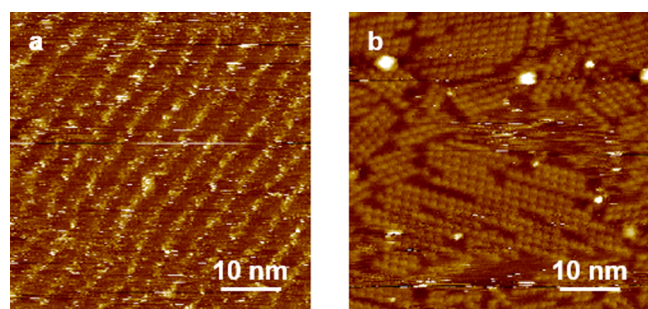


**Figure 5.** STM height images of porphyrin **2b** (1 mM phenyloctane solution): (a) before and (b) after addition of an equimolar amount of Ni(acac)<sub>3</sub>. Tunneling conditions: (a)  $I = 2.0$  pA,  $V = -515$  mV, (b)  $I = 1.3$  pA,  $V = -405$  mV.

198 worlds was reached, i.e. the rapid reversibility of the weak  
199 interactions followed by stable coordination linkages. The  
200 coordination linkages (divalent metal ions + enaminoketone  
201 chelating ligands) used in this study also present the advantage  
202 of adding electronic communication between the subunits in  
203 addition to their connecting role.

## 204 ■ ASSOCIATED CONTENT

### 205 ● Supporting Information

206 The Supporting Information is available free of charge on the  
207 ACS Publications website at DOI: [10.1021/jacs.9b02145](https://doi.org/10.1021/jacs.9b02145).

208 Synthetic procedures, characterization (NMR, mass and  
209 electronic spectra) of all new compounds, X-ray data of  
210 compound **3b**, additional STM images (PDF)  
211 Crystallographic data for **3b** (CIF)

## 212 ■ AUTHOR INFORMATION

### 213 Corresponding Authors

214 \*[rrippert@unistra.fr](mailto:rrippert@unistra.fr)

215 \*[y.kikkawa@aist.go.jp](mailto:y.kikkawa@aist.go.jp)

### 216 ORCID

217 Yoshihiro Kikkawa: [0000-0003-3635-4751](https://orcid.org/0000-0003-3635-4751)

218 Romain Ruppert: [0000-0002-1513-1949](https://orcid.org/0000-0002-1513-1949)

### 219 Notes

220 The authors declare no competing financial interest.

## 221 ■ ACKNOWLEDGMENTS

222 Continuous financial support from the CNRS and the  
223 University of Strasbourg is acknowledged. H.D. thanks the  
224 French Ministry of Research for a PhD fellowship. M.A.C.  
225 thanks the FRC-Labex CSC for her PhD fellowship (ANR-10-  
226 LABX-0026 CSC). Y.K. thanks the JSPS KAKENHI  
227 (17K05851).

## 228 ■ REFERENCES

229 (1) Lehn, J.-M. Toward Self-Organization and Complex Matter.  
230 *Science* **2002**, *295*, 2400–2403.  
231 (2) Whitesides, G. M.; Grzybowski, B. Self-Assembly at All Scales.  
232 *Science* **2002**, *295*, 2418–2421.  
233 (3) Anderson, H. L. Conjugated Porphyrin Ladders. *Inorg. Chem.*  
234 **1994**, *33*, 972–981. Lin, V. S.-Y.; DiMaggio, S. G.; Therien, M. J.  
235 Highly Conjugated, Acetylenyl Bridged Porphyrins: New Models for  
236 Light-Harvesting Antenna Systems. *Science* **1994**, *264*, 1105–1111.  
237 (4) Wang, R.; Brugh, A. M.; Rawson, J.; Therien, M. J.; Forbes, M.  
238 D. E. Alkyne-Bridged Multi[Copper(II) Porphyrin] Structures:  
239 Nuances of Orbital Symmetry in Long-Range, Through-Bond

Mediated, Isotropic Spin Exchange Interactions. *J. Am. Chem. Soc.* **2017**, *139*, 9759–9762. 240  
241  
242 (5) Tsuda, A.; Osuka, A. Fully Conjugated Porphyrin Tapes with  
243 Electronic Absorption Bands That Reach into Infrared. *Science* **2001**,  
244 *293*, 79–82.  
245 (6) Richeter, S.; Jeandon, C.; Gisselbrecht, J.-P.; Ruppert, R.; Callot,  
246 H. J. Syntheses and Optical and Electrochemical Properties of  
247 Porphyrin Dimers Linked by Metal Ions. *J. Am. Chem. Soc.* **2002**, *124*,  
248 6168–6179.  
249 (7) Dekkiche, H.; Buisson, A.; Langlois, A.; Karsenti, P.-L.;  
250 Ruhlmann, L.; Harvey, P. D.; Ruppert, R. Ultrafast Singlet Energy  
251 Transfer in Porphyrin Dyads. *Inorg. Chem.* **2016**, *55*, 10329–10336.  
252 (8) Richeter, S.; Jeandon, C.; Ruppert, R.; Callot, H. J. A Modular  
253 Approach to Porphyrin Oligomers Using Metal Ions as Connectors.  
254 *Chem. Commun.* **2002**, 266–267.  
255 (9) Carvalho, M.-A.; Dekkiche, H.; Karmazin, L.; Sanchez, F.;  
256 Vincent, B.; Kanesato, M.; Kikkawa, Y.; Ruppert, R. Synthesis and  
257 Study at a Solid/Liquid Interface of Porphyrin Dimers Linked by  
258 Metal Ions. *Inorg. Chem.* **2017**, *56*, 15081–15090.  
259 (10) Two recent examples of porphine or porphyrine coupling:  
260 Bischoff, F.; He, Y.; Riss, A.; Seufert, K.; Auwärter, W.; Barth, J. V.  
261 Exploration of Interfacial Porphine Coupling Schemes and Hybrid  
262 Systems by Bond-Resolved Scanning Probe Microscopy. *Angew.*  
263 *Chem., Int. Ed.* **2018**, *57*, 16030–16035. Bengasi, G.; Baba, K.; Frache,  
264 G.; Desport, J.; Gratia, P.; Heinze, K.; Boscher, N. D. Boscher, N. D.  
265 Conductive Fused Porphyrin Tapes on Sensitive Substrates by a  
266 Chemical Vapor Deposition Approach. *Angew. Chem., Int. Ed.* **2019**,  
267 *58*, 2103–2108.  
268 (11) Matena, M.; Riehm, T.; Stöhr, M.; Jung, T. A.; Gade, L.  
269 Transforming Surface Coordination Polymers into Covalent Surface  
270 Polymers: Linked Polycondensed Aromatics through Oligomerization  
271 of N-Heterocyclic Carbene Intermediates. *Angew. Chem., Int. Ed.* **2008**,  
272 *47*, 2414–2417.  
273 (12) Wang, T.; Huang, J.; Lv, H.; Fan, Q.; Feng, L.; Tao, Z.; Ju, H.;  
274 Wu, X.; Tait, S. L.; Zhu, J. Kinetic Strategies for the Formation of  
275 Graphyne Nanowires via Sonogashira Coupling on Ag(111). *J. Am.*  
276 *Chem. Soc.* **2018**, *140*, 13421–13428.  
277 (13) Moreno, C.; Paradinas, M.; Vilas-Varela, M.; Panighel, M.;  
278 Ceballos, G.; Pena, D.; Mugarza, A. On-Surface Synthesis of  
279 Superlattice Arrays of Ultra-Long Graphene Nanoribbons. *Chem.*  
280 *Commun.* **2018**, *54*, 9402–9405.  
281 (14) Shu, C.-H.; Xie, Y.-L.; Wang, A.; Shi, K.-J.; Zhang, W.-F.; Li,  
282 D.-Y.; Liu, P.-N. On-Surface Reactions of Aryl Chloride and  
283 Porphyrin Macrocycles via Merging two Reactive Sites into a Single  
284 Precursor. *Chem. Commun.* **2018**, *54*, 12626–12629.  
285 (15) Haq, S.; Hanke, F.; Dyer, M. S.; Persson, M.; Iavicoli, P.;  
286 Amabilino, D. B.; Raval, R. Clean Coupling of Unfunctionalized  
287 Porphyrins at Surfaces to Give Highly Oriented Organometallic  
288 Oligomers. *J. Am. Chem. Soc.* **2011**, *133*, 12031–12039.  
289 (16) Elemans, J. A. A. W.; Lei, S.; De Feyter, S. Molecular and  
290 Supramolecular Networks on Surfaces: From Two-Dimensional  
291 Crystal Engineering to Reactivity. *Angew. Chem., Int. Ed.* **2009**, *48*,  
292 7298–7332.  
293 (17) Gomar-Nadal, E.; Puigmarti-Luis, J.; Amabilino, D. B. Assembly  
294 of Functional Molecular Nanostructures on Surfaces. *Chem. Soc. Rev.*  
295 **2008**, *37*, 490–504.  
296 (18) Mali, K. S.; Pearce, N.; De Feyter, S.; Champness, N. R.  
297 Frontiers of Supramolecular Chemistry at Solid Surfaces. *Chem. Soc.*  
298 *Rev.* **2017**, *46*, 2520–2542.  
299 (19) Cui, D.; MacLeod, J. M.; Rosei, F. Probing Functional Self-  
300 Assembled Molecular Architectures with Solution/Solid Scanning  
301 Tunneling Microscopy. *Chem. Commun.* **2018**, *54*, 10527–10539.  
302 (20) Binnig, G.; Rohrer, H.; Gerber, C.; Weibel, E. Surface Studies  
303 by Scanning Tunneling Microscopy. *Phys. Rev. Lett.* **1982**, *49*, 57–61.  
304 (21) Stöhr, M. In *Supramolecular Chemistry – Scanning Tunneling*  
305 *Microscopy (STM)*; Gale, P. A., Steed, J. W., Eds.; John Wiley & Sons,  
306 Ltd.: Chichester, 2012; pp 659–668.

- 307 (22) De Feyter, S.; De Schryver, F. C. Self-Assembly at the Liquid/  
308 Solid Interface: STM Reveals. *J. Phys. Chem. B* **2005**, *109*, 4290–  
309 4302.
- 310 (23) Otsuki, J. STM Studies on Porphyrins. *Coord. Chem. Rev.* **2010**,  
311 *254*, 2311–2341.
- 312 (24) Geng, Y.-F.; Li, P.; Li, J.-Z.; Zhang, X.-M.; Zeng, Q.-D.; Wang,  
313 C. STM Probing the Supramolecular Coordination Chemistry on  
314 Solid Surface: Structure, Dynamic, and Reactivity. *Coord. Chem. Rev.*  
315 **2017**, *337*, 145–177.
- 316 (25) Marschall, M.; Reichert, J.; Weber-Bargioni, A.; Seufert, K.;  
317 Auwärter, W.; Klyatskaya, S.; Zoppellaro, G.; Ruben, M.; Barth, J. V.  
318 Random Two-Dimensional String Networks Based on Divergent  
319 Coordination Assembly. *Nat. Chem.* **2010**, *2*, 131–137.
- 320 (26) Heim, D.; Eciija, D.; Seufert, K.; Auwärter, W.; Aurisicchio, C.;  
321 Fabbro, C.; Bonifazi, D.; Barth, J. V. Self-Assembly of Flexible One-  
322 Dimensional Coordination Polymers on Metal Surfaces. *J. Am. Chem.*  
323 *Soc.* **2010**, *132*, 6783–6790.
- 324 (27) Koepf, M.; Wytko, J. A.; Bucher, J.-P.; Weiss, J. Surface-Tuned  
325 Assembly of Porphyrin Coordination Oligomers. *J. Am. Chem. Soc.*  
326 **2008**, *130*, 9994–10001.
- 327 (28) El Garah, M.; Marets, N.; Mauro, M.; Aliprandi, A.; Bonacchi,  
328 S.; De Cola, L.; Ciesielski, A.; Bulach, V.; Hosseini, M. W.; Samori, P.  
329 Nanopatterning of Surfaces with Monometallic and Heterobimetallic  
330 1D Coordination Polymers: A Molecular Tectonics Approach at the  
331 Solid/Liquid Interface. *J. Am. Chem. Soc.* **2015**, *137*, 8450–8459.
- 332 (29) Velpula, G.; Li, M.; Hu, Y.; Zagranyski, Y.; Pisula, W.;  
333 Müllen, K.; Mali, K. S.; De Feyter, S. Hydrogen-Bonded Donor-  
334 Acceptor Arrays at the Solution-Graphite Interface. *Chem. - Eur. J.*  
335 **2018**, *24*, 12071–12077.
- 336 (30) Sun, X.; Fan, L.; Zhou, X.; Tian, W. Q.; Guo, Z.; Li, Z.; Li, X.;  
337 Lei, S. Surface Confined Synthesis of Porphyrin Containing Two-  
338 Dimensional Polymers: The Effect of Rigidity and Preferential  
339 Adsorption of Building Blocks. *Chem. Commun.* **2015**, *51*, 5864–  
340 5867.
- 341 (31) Sakamoto, R.; Takada, K.; Pal, T.; Maeda, H.; Kambe, T.;  
342 Nishihara, H. Coordination Nanosheets (CONASHs): Strategies,  
343 Structures and Functions. *Chem. Commun.* **2017**, *53*, 5781–5801.
- 344 (32) Cai, L.; Sun, Q.; Bao, M.; Ma, H.; Yuan, C.; Xu, W.  
345 Competition between Hydrogen Bonds and Coordination Bonds  
346 Steered by the Surface Molecular Coverage. *ACS Nano* **2017**, *11*,  
347 3727–3732.
- 348 (33) Sosa-Vargas, L.; Kim, E.; Attias, A.-J. Beyond “Decorative” 2D  
349 Supramolecular Self-Assembly: Strategies towards Functional Surfaces  
350 for Nanotechnology. *Mater. Horiz.* **2017**, *4*, 570–583.
- 351 (34) Amabilino, D. B. in *Supramolecular Chemistry at Surfaces.*  
352 *Monographs in Supramolecular Chemistry*; Royal Society of Chemistry,  
353 2016.
- 354 (35) CCDC deposit number: 1893245.
- 355 (36) Shelnutt, J. A.; Song, X.-Z.; Ma, J.-G.; Jia, S.-L.; Jentzen, W.;  
356 Medforth, C. J. Nonplanar Porphyrins and their Significance in  
357 Proteins. *Chem. Soc. Rev.* **1998**, *27*, 31–41.